1986

A Study on Dynamic Behavior of a Scroll Compressor

N. Ishii

M. Fuhushima

K. Sano

K. Sawai

A STUDY ON DYNAMIC BEHAVIOR OF A SCROLL COMPRESSOR

Noriaki Ishii[1],
Masafumi Fukushima[2], Kiyoshi Sano[3] and Kiyoshi Sawai[3]

[1]Professor, Faculty of Engineering, Osaka Electro-Communication University, Neyagawa, Osaka 572, JAPAN
[2]ChiefEngineer,Compressor Division
[3]Chief Engineer, Air Conditioner Division, Matsushita Electric Industrial Co.Ltd. (PANASONIC), Noji-cho, Kusatsu,525, JAPAN

ABSTRACT

This study discusses in relation to compressor dynamics the suitability of a scroll machine for small-sized refrigerant compressors. For this purpose the calculated results on the crankshaft load fluctuation, the crankshaft rotary behavior, the unbalanced inertia forces, the compressor vibrations and the mechanical efficiency of a scroll-type compressor are presented initially. Secondly, the calculated results are compared with those of four different types of compressors: an one-rolling-piston rotary type, a two-rolling-pistons two-blades rotary type, an one-rolling-piston two-blades rotary type and a single-cylinder reciprocating type.

SYMBOLS

B=height of scroll
f_{t1}, f_{t2}=frictional force on thrust-bearing plane
$f_{x1}, f_{x2}, f_{y1}, f_{y2}$=frictional force on Oldam ring
F_i=thrust force due to cylinder pressure
F_0=thrust force due to intermediate pressure
F_x, F_y, F_z=unbalanced force of inertia
F_r=radial gas force
F_t=tangential gas force
F_{t1}, F_{t2}=thrust force on thrust-bearing plane
I_0=crankshaft moment of inertia
I_x, I_y, I_z=compressor moment of inertia
j,k=integer
K=largest number of k
l_e=height of concentrated mass m_e from thrust-bearing plane
l_g=height of orbiting scroll's gravity center
l_0=height of Oldam-slot center
l_q=height of crank-journal center
l_s=height of crank-pin center
L_Q=frictional torque at crank-journal
L_S=frictional torque at crank-pin

m_e=mass of crank-arm, crank-pin & balancers
m_s=mass of orbiting scroll
M=compressor mass
M_m, M_{xm}, M_{ym}=overturning moment
M_0=gas moment
M_{Qx}, M_{Qy}=constraint moment at crank-journal
M_x, M_y, M_z=unbalanced moment of inertia
N=motor torque
O_1, O_2=reaction force at Oldam ring
p_j=gas pressure
p_s, p_d=suction & discharge pressure
Q_x, Q_y=reaction force at crankshaft
r_b=radius of involute base circle
r_e=rotating radius of m_e
r_0=orbiting radius
r_Q=crankshaft radius
r_s=crank-pin radius
R_{or}=radius of Oldam ring
R_{th}=radius of thrust-bearing plane
S_j=area of compression chamber
S_x, S_y=reaction force at crank-pin
t=thickness of scroll
T_1, T_2=reaction force at Oldam ring
x,y=fixed coordinate
x_e, y_e=coordenate of m_e
x_G, y_G, z_G=gravity center of compressor
x_m, y_m=orbiting coordinate
x_r, y_r=coordinate of orbiting scroll center
$\ddot{X}_G$, $\ddot{Y}_G$, $\ddot{Z}_G$=acceleration of compressor translation
η=angle of M_m from x_m axis
θ=orbiting angle
$\ddot{\Theta}_x$, $\ddot{\Theta}_y$, $\ddot{\Theta}_z$=accel ration of compressor rotation
κ=specific heat ratio
μ_0, μ_Q, μ_s, μ_t=coefficient of friction
ϕ=involute angle
$\phi_j(k)$, $\phi_0(k)$=involute angle of contact points of scrolls
ϕ_{je}, ϕ_{0e}=ending involute angle of scroll
ϕ_{j0}, ϕ_{00}=initial angle of involute
ϕ_{js}, ϕ_{0s}=starting involute-angle of scroll

INTRODUCTION

Since air conditioners are often operated in quiet surroundings, the vibration and noise generation of the compressor during steady operation must be minimized. About twelve years ago, the conventional compressors for air conditioners were the reciprocating type. However, recently the one-rolling-piston rotary compressors are used in most low capacity air conditioners. The major reason the reciprocating type compressors were replaced by the rotary type was because of its high volumetric and mechanical efficiency, coupled with its compact, lightweight design. The vibration and noise generation of the rotary compressor has not been so reduced as to satisfy the strict requirement of users sufficiently. The major factor which causes the rotary compressor vibrations is the instantaneous load fluctuation during steady operation. Various methods can be used to overcome this. One is to improve the mechanism of the one-rolling-piston rotary compressor: for instance, to develop a two-rolling-pistons two-blades rotary compressor or an one-rolling-piston two-blades rotary compressor. The other is to design a new mechanism, for instance, a scroll compressor[1-4]. The scroll compressor has many compression chambers which are simultaneously compressed at comparatively low speed.

Therefore, the compressor vibration problems in air conditioners will be considerably alleviated by introducing the scroll compressor.

An important matter is to discover to what degree the introduction of the scroll compressor can alleviate the compressor vibration problems. For this purpose, this study present an analytical method to evaluate the dynamic behavior of the scroll compressor and the calculated results for a scroll compressor of comparatively small capacity. The calculated results are summarized on the gas-torque fluctuation, the crankshaft rotary behavior (speed fluctuation rate and rotary acceleration), the unbalanced inertia forces, the compressor vibrations and the mechanical efficiency. In discussing the suitability of a scroll machine for a small-sized refrigerant compressor, in relation to compressor dynamics, the calculated results for the small scroll compressor are compared with those of the following four types of compressor of similar capacity. The first type is a "1-rotary," namely, an one-rolling-piston rotary, the second a "2-rotary," namely, a two-rolling-pistons two-blades rotary, the third a "2-blades rotary," namely, an one-rolling-piston two-blades rotary and the fourth a "1-recipro.," namely, a single-cylinder reciprocating type.

DESCRIPTION OF SCROLL COMPRESSOR

Fig.1 shows the orbiting-scroll configuration which comprises the two involutes defined by

$$\overline{ST_i} = r_b(\phi - \phi_{i0}),\quad \overline{ST_0} = r_b(\phi - \phi_{00}) \qquad (1)$$

in which φ is the counterclockwise involute-angle from the horizontal x_m-axis. The x_m-y_m coordinate has the origin Om at the center of the basic circle of radius r_b

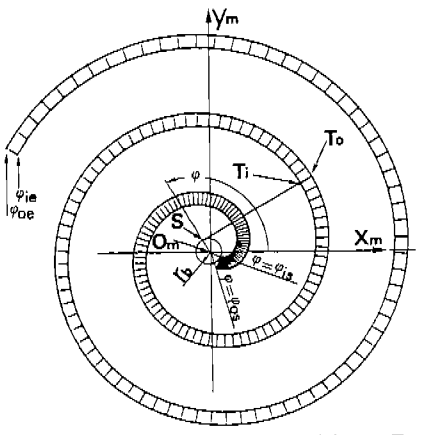

Fig.1 Orbiting scroll

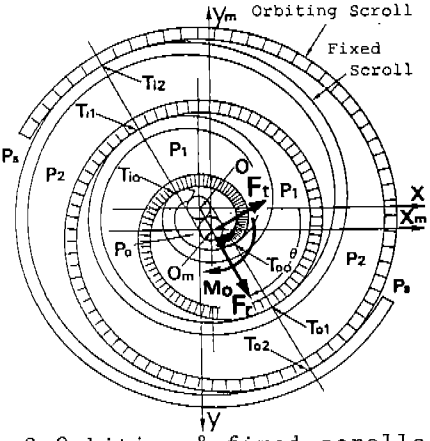

Fig.2 Orbiting & fixed scrolls

and moves with the orbiting scroll. The orbiting scroll is mated with the identical scroll as shown in Fig.2. The non-shadowed scroll is fixed. The basic-circle center O of the fixed scroll is the origin of the static x-y coordinate. The two scrolls touch and form a series of crescent-shaped chamber between two cover-plates, each fixed to the scrolls. The contact points Tik and Tok (k=0,1,...) appear respectively on the two tangents common to the two basic circles. The subscript i and o show respectively the inner and outer contact points of the orbiting scroll. The involute angles $\varphi_i(k)$ and $\varphi_o(k)$ of these contact points are given by

$$\phi_i(k)=2\pi(k+\delta)+3\pi/2-\theta,\quad \phi_o(k)=2\pi(k+\delta)+\pi/2-\theta \qquad (k=0,1,\ldots.) \tag{2}$$

where $\delta=0$ when $0<\theta<\pi/2-\phi_{os}$,

$\delta=1$ when $\pi/2-\phi_{os}<\theta<2\pi$

θ shows the clockwise orbiting angle from the x-axis. The shadowed scroll orbits around the fixed scroll. The orbiting radius r_o is determined by

$$r_o=r_b\pi-t \tag{3}$$

where t is the scroll thickness given by $r_b(\varphi_{io}-\varphi_{oo})$. The orbiting scroll is driven by a motor through an Oldam coupling. The refrigerant of pressure p_s is trapped at the periphery of the scrolls and compressed as the crescent-shaped chambers move toward the center. The compressed refrigerant of pressure p_o is exhausted through the outlet at the fixed-scroll center.

Gas forces acting on the orbiting scroll are reduced to the tangential force Ft which acts against the clockwise orbiting motion, the radial force Fr and the clockwise moment Mo which act on the orbiting-scroll center Om (see Fig. 2). They can be obtained by calculating the following forms.

$$F_t=Br_b\left[\int_{\phi_o(0)}^{\phi_o(K)+\pi}p_j(\phi-\phi_{oo})\cos(\theta+\phi)d\phi-\int_{\phi_i(0)-\pi}^{\phi_i(K)}p_j(\phi-\phi_{io})\cos(\theta+\phi)d\phi\right]-tB(p_o+p_s) \tag{4}$$

$$F_r=-Br_b\left[\int_{\phi_o(0)}^{\phi_o(K)+\pi}p_j(\phi-\phi_{oo})\sin(\theta+\phi)d\phi-\int_{\phi_i(0)-\pi}^{\phi_i(K)}p_j(\phi-\phi_{io})\sin(\theta+\phi)d\phi\right] \tag{5}$$

$$M_o=Br_b^2\left[\int_{\phi_o(0)}^{\phi_o(K)+\pi}p_j(\phi-\phi_{oo})d\phi-\int_{\phi_i(0)-\pi}^{\phi_i(K)}p_j(\phi-\phi_{io})d\phi\right]+tB\left[-\{r_b(\phi_o(0)-\phi_{oo})-t/2\}p_o+\{r_b(\phi_i(K)-\phi_{io})+t/2\}p_s\right] \tag{6}$$

where B represents the height of the scroll. K is the largest number of k. The subscript j of the cylinder pressure changes depending on the integral domain, as follows:

Related to the integral along the outer involute,

$$j=k+1 \text{ when } \phi_0(k)<\phi<\phi_0(k+1) \quad (k=0,1,\ldots,K-1)$$
$$j=K+1 \text{ when } \phi_0(K)<\phi<\phi_0(K)+\pi \qquad (7)$$

Related to the integral along the inner involute,

$$j=0 \quad \text{when } \phi_i(0)-\pi<\phi<\phi_i(0)$$
$$j=k+1 \text{ when } \phi_i(k)<\phi<\phi_i(k+1), \quad (k=0,1,\ldots,K-1) \qquad (8)$$

FUNDAMENTAL EQUATIONS OF MOTION OF MOVING COMPONENTS

Crankshaft System

A crankshaft model is shown in Fig.3 where m_e represents the total mass of the crank-arm, the crank-pin and the balancers, which is concentrated at the gravity point (x_e, y_e) defined by

$$x_e=r_e\cos\theta,\ y_e=r_e\sin\theta \qquad (9)$$

Consider that the motor drive torque N acting around the crankshaft induces the reaction forces Qx, Qy on the crankshaft and the reaction forces Sx, Sy on the crank-pin. Hence, the crankshaft motion in the x and y directions is subjected to the following forms:

$$-m_e\ddot{x}_e-Q_x+S_x=0,\ -m_e\ddot{y}_e+Q_y-S_y=0 \qquad (10)$$

Representing the moment of inertia of the crankshaft system by Io, the equation of rotary motion of the

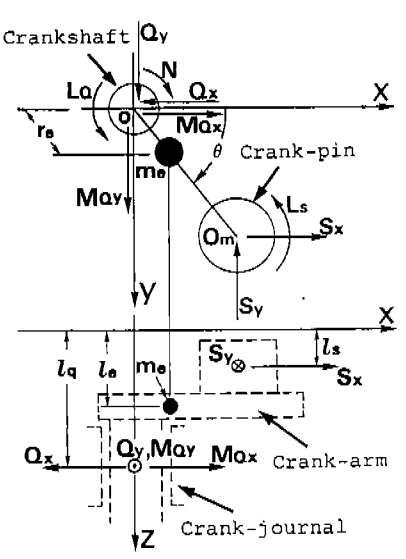

Fig.3 Crankshaft model

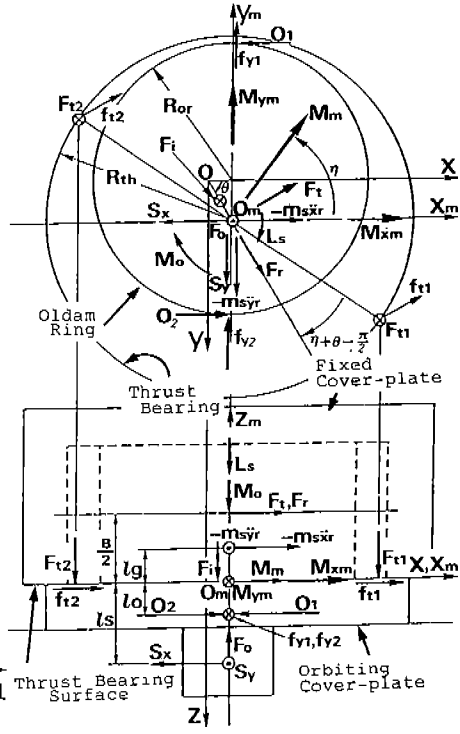

Fig.4 Orbiting-scroll model

crankshaft is given by

$$-I_0\ddot{\theta}-S_x r_0 \sin\theta-S_y r_0 \cos\theta+N-L_Q-L_S=0 \quad (11)$$

L_Q and L_S shows the frictional torque at the crank-journal and the crank-pin respectively which can be evaluated by Coulomb's law of friction as follows:

$$L_Q=\mu_Q\sqrt{Q_x^2+Q_y^2}\times r_Q,\quad L_S=\mu_S\sqrt{S_x^2+S_y^2}\times r_S \quad (12)$$

Representing the reaction moment on the crankshaft from the crank-journal by Mox and Msy, the equilibrium of moment around the x and y axes is given by

$$\begin{aligned} M_{Qy}-S_x(\ell_q-\ell_s)-(-m_e\ddot{x}_e)(\ell_q-\ell_e)=0,\\ M_{Qx}-S_y(\ell_q-\ell_s)+(-m_e\ddot{y}_e)(\ell_q-\ell_e)=0 \end{aligned} \quad (13)$$

Orbiting Scroll

Fig. 4 shows all forces and moments acting on the orbiting scroll. The cross-sectional view along the x_m-z_m plane is also shown to evaluate the thrust forces. It is so designed that the intermediate pressure between the suction and discharge pressure acts on the outer surface of the orbiting cover-plate and hence the orbiting scroll is pressed up toward the fixed cover-plate. The resultant upward force is shown by Fo acting on the center Om. Therefore, the contact plane of the orbiting and fixed cover-plates forms the thrust bearing surface of radius Rth. Consider that the previously defined x-y and x_m-y_m planes coincide with this thrust bearing plane.

The reaction forces produced by the crank-pin on the scroll center Om are represented by Sx and Sy which drive the orbiting scroll. Ft, Fr and Mo are the gas forces and moment given by (4) to (6). O1 and O2 show the reaction forces of the Oldam ring of radius Ror. f_{y1} and f_{y2} are the frictional forces between the Oldam ring and the scroll which are given by the following forms assuming Coulomb's law of friction.

$$f_{y1}=\mu_0|O_1|,\quad f_{y2}=\mu_0|O_2| \quad (14)$$

The resultant thrust force Fi due to the gas pressure in the cylinders acts on the center of the segment $\overline{OO_m}$. The inertia force of the orbiting scroll is represented by $(-m_s\ddot{x}_r)$ and $(-m_s\ddot{y}_r)$, where x_r and y_r are defined by

$$x_r=r_0\cos\theta,\quad y_r=r_0\sin\theta \quad (15)$$

There are forces acting on the orbiting scroll which would tend to force it from the horizontal plane. These forces may best be described as overturning-forces. In order to evaluate the constraint forces at the thrust bearing surface, the moment Mm overturning the orbiting scroll and its counter-clockwise angle η from the x_m axis are derived initially.

$$M_m=\sqrt{M^2_{xm}+M^2_{ym}},\quad \eta=\tan^{-1}(M_{ym}/M_{xm}) \quad (16)$$

where Mxm and Mym representing the momentcomponents around the x_m and y_m axes are given by

$$\begin{aligned} M_{xm}=&-F_i\cdot y_r/2-F_t\cos\theta\cdot B/2+F_r\sin\theta\cdot B/2\\ &+(-m_s\ddot{y}_r)\ell_g+(f_{y1}+f_{y2})\ell_0-S_y\ell_s, \end{aligned} \quad (17\text{-}1)$$

$$M_{ym}=-F_i\cdot x_r/2+F_t\sin\theta\cdot B/2+F_r\cos\theta\cdot B/2 +(-m_s\ddot{x}_r)\ell_s+(O_1-O_2)\ell_0+S_x\ell_s \quad (17\text{-}2)$$

This overturning moment Mm must be supported by the thrust bearing surface. In order to simplify the analysis, assume that Mm is supported at the two representative points on both the thrust-bearing circle and the line perpendicular to Mm passing Om. Under this assumption, the reaction thrust-forces Ft1 and Ft2 at these two points are given by

$$F_{t1}=(-M_m/R_{th}-F_i+F_0)/2,\ F_{t2}=(M_m/R_{th}-F_i+F_0)/2 \quad (18)$$

Therefore the frictional forces f_{t1} and f_{t2} at these points are given by the following forms, assuming Coulomb's law of friction.

$$f_{t1}=\mu_t|F_{t1}|,\ f_{t2}=\mu_t|F_{t2}| \quad (19)$$

The direction of these frictional forces is perpendicular to the segment 00m.

Since the forces acting on the orbiting scroll can be defined, the equation of motion can be derived. The equations of motion in the x and y directions are given by

$$\begin{aligned}&(-m_s\ddot{x}_r)-S_x+(F_t+f_{t1}+f_{t2})\sin\theta+F_r\cos\theta-O_1+O_2=0,\\&(-m_s\ddot{y}_r)+S_y+(-F_t-f_{t1}-f_{t2})\cos\theta+F_r\sin\theta-f_{y1}-f_{y2}=0\end{aligned} \quad (20)$$

The moment around the z axis is balanced by the reaction moment due to the Oldam ring as follows:

$$M_0-L_S-(f_{t1}-f_{t2})R_{th}\sin(\eta+\theta)=O_1(R_{or}+y_r)+O_2(R_{or}-y_r) \quad (21)$$

Oldam ring

A model of the Oldam ring which performsreciprocating motion along the x direction is shown in Fig. 5. The mass m_o of the Oldam ring is concentrated at its center $(x_r,0)$. O1 and O2 are the reaction forces of the orbiting scroll. f_{y1} and f_{y2} are the frictional forces given by (14). T1 and T2 are the reaction forces of the guide slot fixed on the compressor body. f_{x1} and f_{x2} represent the frictional forces between the guide slot and the Oldam ring, which are given by

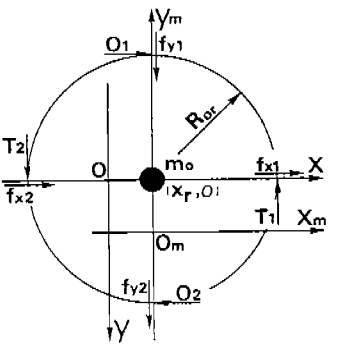

Fig.5 Oldam-ring model

$$f_{x1}=\mu_o|T_1|,\ f_{x2}=\mu_o|T_2| \quad (22)$$

By defining the forces acting on the Oldam ring, the equation of motion in the x direction can be given by

$$(-m_0\ddot{x}_r)+O_1-O_2+f_{x1}+f_{x2}=0 \quad (23)$$

The equilibrium equations of forces in the y axis and of moment around the Oldam ring center are respectively prescribed by

$$-T_1+T_2+f_{y1}+f_{y2}=0,\ O_1+O_2-T_1-T_2=0 \quad (24)$$

EQUATION OF ROTARY MOTION OF CRANKSHAFT

Rearranging the fundamental equations of motion of the moving components, all constraint forces and moments can be derived as a function of the orbiting angle θ. Substituting the derived constraint-forces Sx and Sy into (11), the equation of rotary motion of the crankshaft can be rewritten in the following form.

$$(I_0+m_s r_0^2+m_0 r_0^2\sin^2\theta)\ddot{\theta}+m_0 r_0^2\sin\theta\cdot\cos\theta\cdot\dot{\theta}^2=N-\{F_t r_0+L_Q+L_S+(f_{x1}+f_{x2})r_0\sin\theta+(f_{y1}+f_{y2})r_0\cos\theta+(f_{t1}+f_{t2})r_0\} \quad (25)$$

The left side represents the moments of inertia. The first moment on the right side is the drive torque and the second represents the load torques. The first load torque is due to gas compression and the others are due to mechanical frictions on each pair of machine components.

EXCITING FORCES AND MOMENTS, AND COMPRESSOR VIBRATIONS

In order to discuss the compressor vibration, the exciting forces and moments of the compressor body should be derived initially. Since the forces and moments acting on the moving components have been indicated in the previous section, it is not difficult to calculate the forces and moments acting on the compressor body. The summation of these forces and moments gives the following expressions, namely, unbalanced forces and moments of inertia.

$$\begin{aligned}
&F_x=-(m_e r_e/r_0+m_s+m_0)\ddot{x}_r \rightarrow -(m_0/2)\ddot{x}_r,\\
&F_y=-(m_e r_e/r_0-m_s)\ddot{y}_r \rightarrow -(m_0/2)\ddot{y}_r,\quad F_z=0,\\
&M_x=(m_e r_e\ell_e/r_0-m_s\ell_s)\ddot{y}_r \rightarrow -(m_0/2)\ell_0\ddot{y}_r,\\
&M_y=(-m_e r_e\ell_e/r_0+m_s\ell_s-m_0\ell_0)\ddot{x}_r \rightarrow -(m_0/2)\ell_0\ddot{x}_r,\\
&M_z=-(I_0+m_s r_0^2)\ddot{\theta}
\end{aligned} \quad (26)$$

in which the best static balancing and the best dynamic balancing have been achieved by choosing optimum values of m_e, r_e and l_e. Fx, Fy and Fz are the forces acting on the point O. Mx, My and Mz are the moments around the x, y and z axes respectively.

Assume that the natural vibration frequencies of the compressor elastically suspended by coiled springs are fairly small compared with the mean rotation speed of the crankshaft. Thus, the compressor vibrations can be approximately calculated from the following simple expression.

$$[\ddot{X}]=[M]^{-1}[E][F] \quad (27)$$

where

$$[X]=\begin{bmatrix}X_G\\Y_G\\Z_G\\\Theta_x\\\Theta_y\\\Theta_z\end{bmatrix},\ [M]=\begin{bmatrix}M&\cdots&\cdots&0\\\cdot&M&&\cdot\\\cdot&&M&\cdot\\\cdot&&&I_x\ \cdot\\\cdot&&&\quad I_y\cdot\\0&\cdots&\cdots&I_z\end{bmatrix},\ [E]=\begin{bmatrix}1&\cdots&\cdots&0\\0&1&&\cdot\\0&0&1&\cdot\\0&z_G&-y_G&1\ \cdot\\-z_G&0&x_G&0\ 1\ \cdot\\y_G&-x_G&0&0\ 0\ 1\end{bmatrix},\ [F]=\begin{bmatrix}F_x\\F_y\\F_z\\M_x\\M_y\\M_z\end{bmatrix} \quad (28)$$

SPECIFICATION OF SCROLL COMPRESSOR FOR NUMERICAL CALCULATION

Table 1 gives the specification of scroll configuration. Since the initial angles of the inner and outer involutes with a base circle of radius 0.2069 cm are 0° and -110.77° respectively, the scroll thickness is 0.4 cm and hence the orbiting radius is 0.25 cm from (3). The scrolling number of the involutes is 2.5. Fig.6 shows the calculated area Sj(j=0,1,2) of the identical crescent-shaped compression-chambers. This figure shows the change in area for about two revolutions of the crankshaft. As θ increases, the suction area of 8.796 cm trapped at the periphery of the scrolls decreases linearly until the two identical compression chambers are connected at θ=117.6°. Assume that the gas-compression process is subjected to the adiabatic change of specific heat ratio 1.32. Thus, the compression-chamber gas pressure p_j shown in Fig.7 can be calculated from Fig.6. Consider that the scroll compressor has no valve at the discharge port. Hence the discharge pressure is approximately determined by the compression-chamber pressure just when the two identical chambers are connected at θ=117.16°. Thus, thegas pressure increases from the given suction pressure 0.617 MPa to the discharge 2.17 MPa. Finally consider that the intermediate pressure p_{md} pressing the orbiting scroll up toward the fixed scroll is 0.882 MPa.

Tab.1 Specification of scroll

B	=1.166 cm
r_b	=0.2069 cm
r_o	=0.25 cm
t	=0.4 cm
ϕ_{i0}	=0°
ϕ_{00}	=−110.77°
ϕ_{is}	=0°
ϕ_{0s}	=−27.16°
ϕ_{ie}	=900.0°
ϕ_{oe}	=900.0°

Table 2 shows the major mechanical constants of a small-sized scroll compressor presently being developed. Assume that the friction coefficients at each pair of moving components take the same value of 0.027 which was determined on the basis of the previous studies [5,6] carried out using a 1-rotary compressor. The scroll

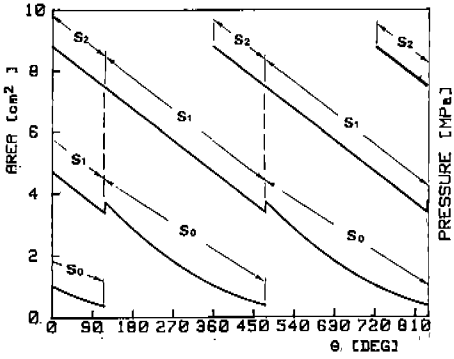

Fig.6 Crescent-shaped area Sj

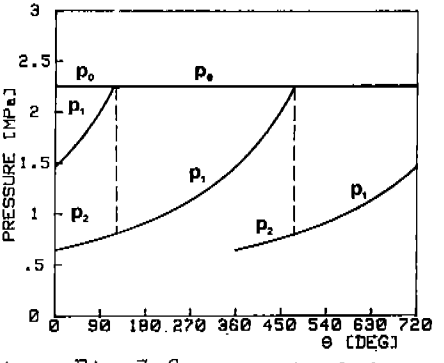

Fig.7 Gas pressure p_j

Tab.2 Mechanical constants of scroll compressor

I_0 =0.0422 N·cm·s^2	m_s =0.277 Kg
I_x =3.519 N·cm·s^2	r_e =-0.101 cm
I_y =3.904 N·cm·s^2	R_{or}=2.85 cm
I_z =0.996 N·cm·s^2	r_Q=1.0 cm
ℓ_e=-0.4003 cm	r_s =1.0 cm
ℓ_s=0.5 cm	R_{th}=4.1 cm
ℓ_o=0.7 cm	v_s =10.26 cm^3
ℓ_q=4.6 cm	x_G =0 cm
ℓ_s=1.9 cm	y_G =0 cm
M =8.7 Kg	z_G =6.54 cm
m_e =0.746 Kg	μ_o, μ_Q, μ_S, μ_t
m_o =0.051 Kg	=0.027

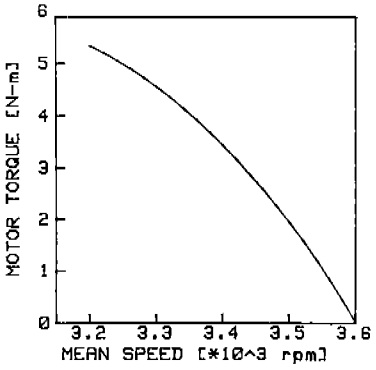

Fig.8 Motor torque curve

compressor is driven by the motor torque shown in Fig. 8. The synchronous speed is 3600 rpm.

COMPARISON OF OTHER REFRIGERANT COMPRESSOR TYPES

For clarity of understanding, the calculated results on the scroll-compressor's dynamic behavior may be compared with those of the other types of refrigerant compressor. Comparisons of a 1-rotary, a 2-rotary, a 2-blade rotary and a 1-recipro. type compressors are made. Of course, they must be of the same capacity as the scroll compressor, that is, their suction-gas volume should be about 10.26cm . For comparison of the compressor vibrations and the mechanical efficiency, it should be, moreover, assumed that the major mechanical constants, for instance, the rotating-crankshaft moment of inertia, the compressor mass, the compressor moment of inertia, the compressor-gravity coordinate and the friction coefficients take the same values as those in Table 2 of the scroll compressor, respectively.

Please refer to the previous studies [5,6] for the 1-rotary compressor of the same capacity and mechanical constants as the scroll compressor. The 1-rotary compressor is composed of a rolling piston, a blade, a cylinder and a crankshaft. The diameter, the mass and the eccentricity of the rolling piston are 3.24mm, 0.0741Kg and 3.3mm respectively. The blade mass is 0.0113 Kg. The diameter and the depth of the cylinder are 3.9cm and 2.8cm respectively. On the basis of this 1-rotary compressor, the 2-rotary and the 2-blade rotary compressors can be developed. Assume that the cylinder spaces are equally divided by setting a thin partition plate at the center of the cylinder depth and the eccentricity directions of the divided two rolling-

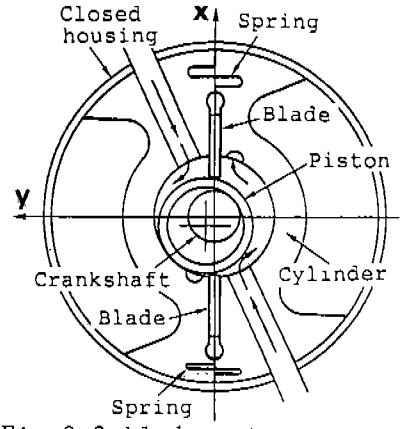

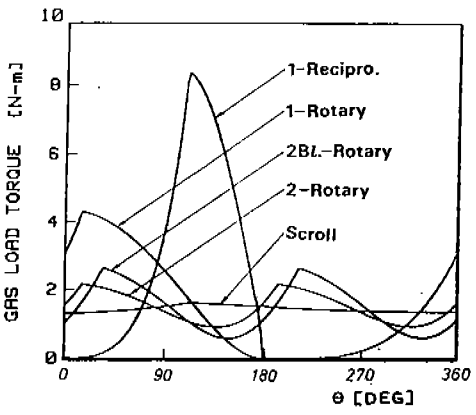

Fig.9 2-blade rotary compressor Fig.10 Gas-load torque

pistons are opposite. Hence the two blades perform reciprocating motion in opposite directions. This type of compressor possessing two rolling-pistons and two blades is called "2-rotary." A cross-sectional view of the 2-blade rotary is shown in Fig. 9. The difference from the 1-rotary is that the 2-blade rotary has one extra blade. The two blades perform the same reciprocating motion. Please refer to the previous studies [7-11] for the compressor dynamics on the conventional 1-reciprocating type. The 1-recipro. compressor of the same capacity has a piston of diameter 2.48cm and mass 0.16Kg, and a 4.24cm long connecting-rod of mass 0.053Kg. The rotating crank radius is 1.06cm.

CALCULATED DYNAMIC BEHAVIOR OF SCROLL COMPRESSOR COMPARED WITH OTHER TYPES OF COMPRESSOR

Substituting the compression-chamber gas pressure shown in Fig. 7 into (4) to (6), the gas forces Ft, Fr and moment Mo acting on the orbiting scroll can be calculated. Hence, the gas torque F r on the right side of (25) is obtained as shown in Fig. 10 which includes the calculated gas torques of the other four types. The cylinder pressure of the other four types was also calculated assuming the adiabatic change of specific heat ratio 1.32. The same pressure 0.617MPa as the scroll compressor was chosen for the suction pressure. The average gas-load for the other four types should be, of course, the same as the scroll compressor. Therefore the discharge pressure of the other four types was so adjusted that the gas compression-work per crankshaft-revolution takes the same value 9.30Nm as the scroll compressor. It is important to find the fluctuation magnitudes of the gas torques from Fig. 10. They are shown on the second line of Table 3. The standard decibel values in parentheses are those of the 1-rotary

compressor which is, at present, most commonly used for air-conditioning appliances. The gas torque fluctuation of the scroll compressor is the lowest -22.8 dB. This level is lower by 12.1 dB compared with the 2-rotary which is the second lowest. This is an excellent characteristic of the scroll compressor, which is results from the fact that many compression chambers are compressed simultaneously. The third lowest is the 2-blade rotary, the forth is the 1-rotary and the worst is the 1-recipro. type.

The crankshaft motion of the scroll compressor can be numerically calculated from (25), applying a repeated calculation method. The calculated results of the average crankshaft-speed and the speed fluctuation ratio are shown in Table 3. The crankshaft-speed fluctuation ratio of the scroll compressor is very small. Its value of 0.50 is about half that of the 2-rotary type. The calculated $\ddot{\theta}$ is shown in Fig. 11 which includes those of the other four types. Using the calculated $\ddot{\theta}$, the exciting moment Mz is calculated from the sixth form of (26) and thus (27) gives the rotation acceleration $\ddot{\Theta}_z$ of the compressor body which is shown in Fig. 12. The peak to peak values of $\ddot{\theta}$ and $\ddot{\Theta}_z$ are summarized in Table 3. From these results it is confirmed that the fluctuation levels of $\ddot{\theta}$ and $\ddot{\Theta}_z$ are smallest for the scroll compressor and increase by a similar rate as the gas-torque fluctuation becomes larger. It may be concluded

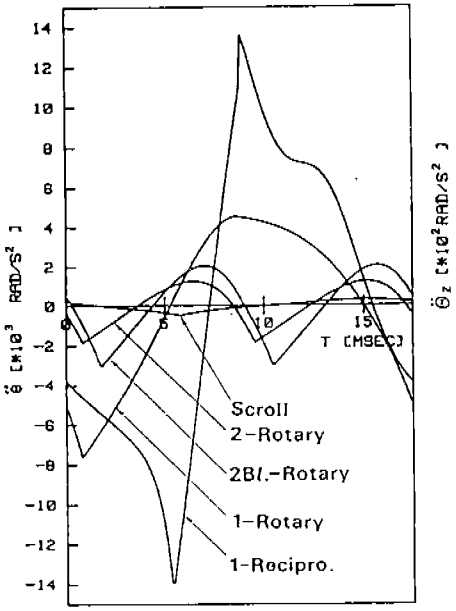

Fig.11 Rotatory acceleration of crankshaft

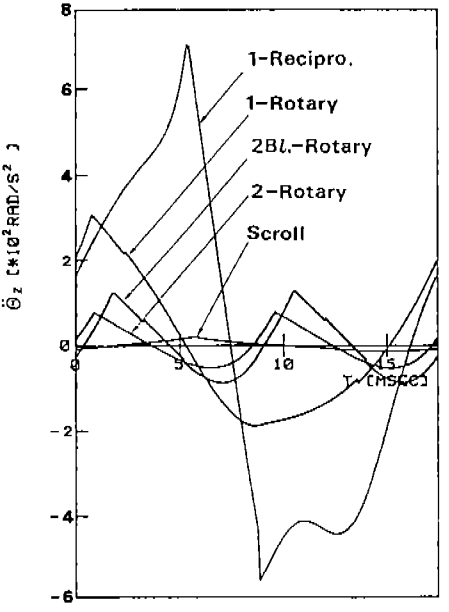

Fig.12 Compressor-body acceleration around crankshaft

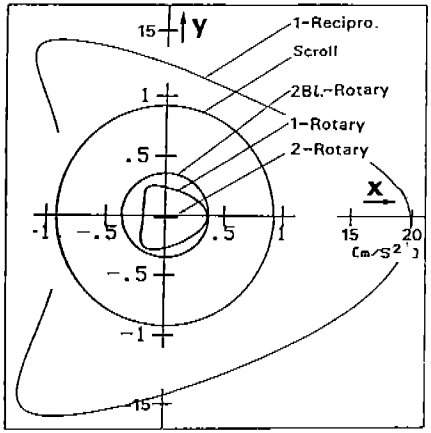

Fig.13 Vector trajectories of translation accelerations

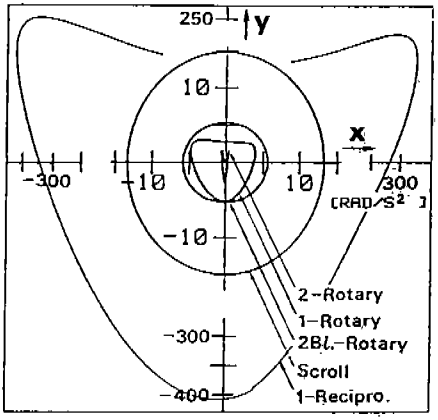

Fig.14 Vector trajectories of rotation accelerations

that the scroll compressor is significantly improved in $\ddot{\theta}$ and $\ddot{\Theta}_z$ compared with the 1-rotary type and, even compared with the 2-rotary or the 2-blade rotary. These fluctuation levels are lower by 11dB to 16dB.

Using the calculated $\ddot{\theta}$, the exciting forces Fx, Fy and moments Mx, My are calculated from (26) and thus (27) gives the compressor translation-accelerations $\ddot{X}_G$, and $\ddot{Y}_G$ and rotation accelerations $\vec{\ddot{\Theta}}_x$, $\vec{\ddot{\Theta}}_y$. The translation and rotation accelerations are shown by trajectories of vectors $(\vec{\ddot{X}}_G + \vec{\ddot{Y}}_G)$ in Fig.13 and vectors $(\vec{\ddot{\Theta}}_x + \vec{\ddot{\Theta}}_y)$ in Fig. 14. The x and y axes correspond to the axes in Fig. 2 for the scroll type and the axes in Fig. 9 for the rotary types. For the 1-recipro., the piston center line coincides with the x axis. These figures represent the degree of static and dynamic balancing and also the crankshaft-speed fluctuation. The vector trajectories of the 1-rotary and the 1-recipro. are comparable to a rough triangle, since their speed fluctuation ratios are fairly large. As the speed fluctuation ratio decreases, like the scroll, and the 2-blade rotary types, the vector trajectories approach a circle. In the case of the 2-rotary type, the static balancing is achieved ideally, i.e. the static unbalanced forces of inertia are reduced to zero. The vector trajectory of a short segment in Fig. 13 results from the second-order unbalanced forces of inertia, and these mainly cause the 2-rotary type's vector trajectory shown in Fig. 14. The well dynamic balancing of the 2-rotary type can also be achieved since the acceleration amplitude caused by the first-order unbalanced moments of inertia is about 0.45 rad/s . The maximum values of each vector-trajectory are summarized in Table 3. The scroll compressor is worse in both static and dynamic balancing even compared

with the 1-rotary or the 2-blade rotary. The major reason is that the scroll compressor has the Oldam coupling ring of larger mass which is about 4.5 times the blade mass of the 1-rotary.

Next consider which type of compressor possesses the most well-balanced characteristic in relation to compressor vibrations. It is evident that the most-commonly used 1-rotary type is fairly good in relation to vibrations, compared with the 1-recipro. type. However, the vibration $\ddot{\Theta}_z$ (=507 rad/s^2) around the rotating crankshaft is much larger than the others $\vec{\ddot{\Theta}}_x + \vec{\ddot{\Theta}}_y$ (=5.12 rad/s^2). The 2-rotary type is good in relation to vibration $\ddot{\Theta}_z$ but it may not be satisfactory enough for the user's exact requirements. In the case of the scroll type, the vibration $\ddot{\Theta}_z$ is greatly reduced to 35.5 rad/s^2 which is of the same order as $\vec{\ddot{\Theta}}_x + \vec{\ddot{\Theta}}_y$. From this point of view, it may be concluded that the scroll type possesses a revolutionary well-balanced characteristic in relation to compressor vibrations, though both the static and dynamic balancing is never better than the rotary types.

The calculated values of mechanical efficiency are shown on the last line of Table 3. Compared with the high efficiency of the rotary types, the mechanical efficiency of the scroll type is lower by 10.8% to 12%. This difference results from the following. The first is that the lubrication at the pair of crank-pin and piston is under fluid friction for the rotary types and on the other hand under Coulomb friction for the scroll type. The second is that the scroll type has an extra thrust-bearing supporting a fairly large thrust force, which causes extra energy consumption due to mechanical friction.

Tab. 3 Major characteristics of five refrigerant compressors

compressor type	scroll	1-rotary	2-rotary	2-blades rotary	1-recipro.
p-p value of gas torque (Nm)	0.31 (-22.8dB)	4.30	1.26 (-10.7dB)	2.07 (-6.4dB)	8.38 (+5.8dB)
average crankshaft-speed(rpm)	3385	3404	3422	3429	3469
speed fluctuation ratio (%)	0.50	8.24	1.06	1.78	15.0
p-p value of $\ddot{\theta}$ (rad/s^2)	794 (-23.7dB)	12200	3100 (-11.9dB)	5070 (-7.6dB)	27500 (+7.1dB)
p-p value of $\ddot{\Theta}_z$ (rad/s^2)	35.5 (-23.1dB)	507	132 (-11.7dB)	218 (-7.3dB)	1280 (+8.0dB)
max. of $(\vec{\ddot{X}}_G + \vec{\ddot{Y}}_G)$ (m/s^2)	0.94 (+8.6dB)	0.35	0.09 (-11.9dB)	0.37 (+0.5dB)	19.8 (+35.1dB)
max. of $(\vec{\ddot{\Theta}}_x + \vec{\ddot{\Theta}}_y)$ (rad/s^2)	14.9 (+9.3dB)	5.12	2.62 (-5.8dB)	5.73 (+1.0dB)	425 (+38.4dB)
mechanical efficiency (%)	80.0	90.8	91.8	92.0	77.9

CONCLUSION

An analytical method to evaluate the scroll compressor's dynamic behavior was established. Calculation was performed for the comparatively small-sized scroll compressor of suction-gas volume 10.26cm and the calculated results were compared with those of the 1-rotary, the 2-rotary, the 2-blade rotary and the 1-recipro. type compressors of the same capacity and similar major mechanical constants. We may conclude from this study as follows:

(1) The introduction of the scroll compressor can reduce the main vibration component, that is, the vibration around the rotating crankshaft by 23.1dB compared with the 1-rotary type, 11.8dB compared with the 2-rotary type, 16.1dB compared with the 2-blade rotary type and 30.8dB compared with the 1-recipro. type. Therefore it may be concluded that the scroll compressor can significantly alleviate the vibration problems commonly found in the other types of compressors.

(2) The mechanical efficiency of the scroll compressor is lower by 10.8 to 12.8% than the rotary type compressors. To overcome this bad characteristic, a special device for lubrication is desirable for the scroll compressors.

ACKNOWLEDGEMENT

The authors would like to express their great thanks to Mr. Kazuhiko Sugiyama, Head of Compressor Division, Mr. Hisao Ohuchi and Mr. Michio Yamamura, Directors of Air-Conditioner Division, Matsushita Electric Industrial Co. Ltd., for their financial support in carrying out this work and their permission to publish this work. They also wish to express their sincere thanks to Chief Hiroshi Morokosi, Chief Shigeru Muramatsu for their help in completing this paper and Mr. Teruhisa Yagura for his help in carrying out the computer calculation of this study.

REFERENCES

1. Moore, R.W., et al., "A Scroll Compressor for Shipboard Helium Liquefier Systems," Purdue Compressor Technology Conference, July 1976, pp. 417-422.
2. McCullough, J.E. and Hirschfeld, F., "The Scroll Machine - An Old Principle with a New Twist," Journal of Mechanical Engineering, Dec. 1979, pp. 46-51.
3. Sugihara, M., et al.,"Scroll Compressor Analytical Model," Proc, of the 1984 Intern. Compr. Engrg. Conference (Purdue), July 1984, pp. 487-495.

4. Tojo, K., et al.,"A Scroll Compressor for Air Conditioners," Proc. of the 1984 Intern. Compr. Engrg. Conf. (Purdue), July 1984, pp. 496-503.
5. Imaichi, K., et al., "Vibration Analysis of Rotary Compressors," Proc. of the Purdue Compr. Technology Conference, July 1982, pp. 275-282.
6. Ishii, N., et al., "The Study of Rolling Piston, Rotary Compressor Dynamic Behavior when Stopping to Reduce Noise and Vibration Level," Proc. of Intern. Compr. Engrg. Conference (Purdue), July 1984, pp.259-266.
7. Imaichi, K., et al., "Vibration of a Small Reciprocating Compressor," ASME Paper 75-DET-44, 1975, Washington, D.C..
8. Imaichi, K., et al., "Leakage Effects on Indicator Diagram at Stopping of Reciprocating Compressors," Proc. of the Purdue Compr. Technology Conference, July 1978, pp. 283-288.
9. Imaichi, K., et al., "A Device for Stopping Single-Cylinder Reciprocating Compressors Silently by Greatly Reducing Vibrations," Proc. of the XVth Intern. Congr. of Refrigeration , Sept. 1979, pp. 727-733.
10. Ishii, N., et al.,"A Computer Simulation of Higher Frequency Vibrations of a Reciprocating Compressor," Proc. of the 16th Intern. Congr. of Refrigeration, Paris, Sep. 1983, pp. 418-423.
11. Imaichi, K., et al., "A Vibration Source in Refrigerant Compressors," Trans. of ASME: Journal of Vibration, Acoustics, Stress and Reliability in Design, Vol. 106, 1984, pp. 122-128.